Available online at www.sciencedirect.com
SCIENCE DIRECT®
Scripta Materialia 53 (2005) 949–954
Scripta MATERIALIA
www.actamat-journals.com

Gallium-doped silicon nitride nanowires sheathed with amorphous silicon oxynitride

Congkang Xu [a], Misuk Kim [a], Junghwan Chun [a], Dong Eon Kim [a,*], Bonghwan Chon [b], Sangsu Hong [b], Taiha Joo [b]

[a] *Department of Physics and Electron Spin Science Center, Pohang University of Science and Technology, Pohang 790-784, Korea*
[b] *Department of Chemistry, Pohang University of Science and Technology, Pohang 790-784, Korea*

Received 29 April 2005; received in revised form 7 June 2005; accepted 17 June 2005
Available online 12 July 2005

Abstract

Gallium-doped silicon nitride nanowires sheathed with amorphous silicon oxynitride have been prepared on silicon substrates using GaN as the source of Ga. Ga plays important roles not only in the formation of silicon nitride nanowires but also their oxidation, forming the sheath of silicon oxynitride. The as-grown nanowires are of significance in facilitating complementary metal-oxide semiconductor-based nanodevice manufacturing. The photoluminescence spectra of the nanowires at 10 K and 300 K are also investigated.

Keywords: Chemical vapor deposition (CVD); High-resolution transmission electronic microscope (HRTEM)

1. Introduction

Silicon nitride and oxynitride (more accurately, nitrogen-doped SiO_2) are appealing for diverse applications. Due to its remarkable electrical, optical and chemical properties, such as larger dielectric constant, larger refractive index, high hardness, chemical inertness, good corrosion, and high thermal stability [1–3], silicon nitride can be widely applied in protective coatings against wear and corrosion [4], microelectronic devices, anti-diffusion barriers [5], and anti-reflection coatings for solar cells [6]. On the other hand, the chemical and mechanical properties of high dopant concentration silicon nitride are similar to GaN and AlN, which have been employed to grow quantum well structures so as to obtain blue lasers. The high Er concentration (~10 at.%) in SiN_x films [7] may be extended to the construction of hybrid electro-optical devices. Like silicon nitride films, silicon oxynitride, which is the leading candidate to substitute for SiO_2, is one of the most important dielectric materials [8–10]. Silicon oxynitrides (SiO_xN_y) thin films are of interest for gate dielectrics and ultralarge scale integrated circuits [11–13]. Since the dielectric constant of oxynitride increases linearly with the concentration of nitrogen from SiO_2 ($\varepsilon = 3.8$) to Si_3N_4 ($\varepsilon = 7.8$) [14] the performance of CMOS (complementary metal-oxide semiconductor)-based devices [15–17] largely depends upon the nitrogen concentration in silicon oxynitride. High concentration of nitrogen in silicon oxynitride is generally expected; however, most of SiO_xN_y films studied up to now have nitrogen concentration less than 10 at.% and therefore have a dielectric constant only slightly higher than that of pure SiO_2. Additionally, boron- and phosphorus-doped silicon oxynitride is of importance and significance for CMOS manufacturing. Hence, new element doped silicon oxynitride such as

* Corresponding author.
E-mail addresses: ckxu@postech.ac.kr (C. Xu), kimd@postech.ac.kr (D.E. Kim).

1359-6462/$ - see front matter © 2005 Acta Materialia Inc. Published by Elsevier Ltd. All rights reserved.
doi:10.1016/j.scriptamat.2005.06.024

Ga-doped SiO_xN_y is expected to have more advantageous performance. A great deal of attention is currently being paid to the fabrication of low dimensional nanomaterials, such as nanowires, nanotubes and nanocables, as a consequence of their unique properties and diverse potential applications in nanodevices. Of these low dimensional nanomaterials, silicon oxynitride nanowires are much favored for CMOS-based devices. In the past decades, the approach to fabrication of silicon oxynitride has been in general to dope nitrogen into silica, which makes it difficult to attain high nitrogen concentration silicon oxynitride. However, to our knowledge, no literature on Ga-doped silicon nitride nanowires is available, not to mention Ga-doped silicon nitride nanowires sheathed with silicon oxynitride.

This article reports an effort to prepare Ga-doped silicon nitrides nanocables, which enables us to tailor the properties of silicon nitride and silicon oxynitride, and improve the performance of CMOS-based devices. We successfully realized the doping of Ga into silicon nitride nanowires and attained the Ga-doped silicon nitride nanocables.

2. Experimental

GaN powders (99.99%, Sigma Aldrich) were used as a source for Ga, Ar 95% + H_2, and NH_3 were used as both carrier gas and reacting gas. Either pure Si substrates or 0.6 nm-thickness Au-coated silicon substrates were used after having been cleaned ultrasonically in acetone for 30 min.

A quartz boat containing reagent grade GaN powder (Aldrich, 99.99%) was kept in the center of a quartz tube placed horizontally in a tubular furnace. A cleaned silicon substrate was placed downstream from the boat. The distance between the boat and substrate was 150 mm. The base vacuum was kept at 95 mTorr. The powder was heated up to 900 °C at a rate of 15 °C/min with a flow of Ar 95% + H_2 5% at 60 sccm. Ar + H_2 gas was then turned off, and a pure ammonia gas (99.999%) was introduced at 50 sccm. The furnace was then heated up to 1050 °C at a rate of 10 °C/min and held for 300 min, and the substrate temperature was about 980 °C. The reaction chamber pressure was kept at 300 mTorr. After the furnace was cooled down to ambient temperature with NH_3, the sample was obtained from the substrate.

As-prepared samples were characterized by X-ray diffraction (XRD, RIGAKU D/MAX-IIA) with CuK_α radiation. The morphology and size distribution of the nanowires were characterized using a scanning electronic microscope (SEM, HitachiH-8010) equipped with energy-dispersive X-ray (EDX) spectroscopy and a transmission electronic microscope (TEM, Hitachi H-800). High-resolution TEM (HRTEM), EDX, selected area electron diffraction (SAED) and line-scan analyses were performed with a JEOL-2010. The laser at 266 nm was used as an excitation source in the photoluminescence (PL) measurements.

3. Results and discussion

Fig. 1(a) shows the SEM image of as-prepared samples grown on a silicon substrate with GaN powder. Most of the nanowires have spearlike tips. The diameters of the nanowires range from 50 nm to 200 nm, and the lengths reach up to tens of microns. The length of the spearlike tip is about 3 μm. EDX analyses (lower inset) indicate that the nanowires consist of Si, N and Ga with the atomic ratio of 78:19.4:2.6; the Ga content of the nanowires is about 3 at.%. Some nanowires not only contain Si, N and Ga but also O. The content of oxygen in the nanowires varies with different nanowires. Note that the Si source is directly from the substrate. These nanowires are probably dominated by the recombination of vapor–liquid–solid (VLS) and solid–liquid–solid (SLS).

Fig. 1(b) demonstrates the SEM image of as-prepared samples grown on the gold-coated silicon substrate without GaN under the same conditions as that of Fig. 1(a). The nanowires have the diameters ranging from 30 to 220 nm. EDX analysis indicates that they are composed of Si and N with the atomic ratio of 65:35, and Si is rich in the nanowires. No obvious oxygen element is detected.

The irregular round tips are Au–Si alloys, different from spear-like tips on pure Si substrate. These nanowires are most likely to be formed by VLS mechanism.

Fig. 2 represents the XRD pattern of as-prepared samples. The prominent seven diffraction peaks correspond to (101), (110), (200), (002), (102), (210) and $(\bar{2}\bar{1}1)$ planes of a bulk α-Si_3N_4 with hexagonal structure ($a = 7.765$ Å, $c = 5.627$ Å). The majority of the sample is hexagonal α-Si_3N_4.

Fig. 3(a) shows the TEM image of a nanowire with a spearlike tip grown on a silicon substrate. The composition of a nanowire was probed by EDX attached to TEM. The EDX analysis (lower inset) shows that the nanowire is composed of Si, N and Ga with the atomic ration of 65:33:2, the atomic ratio of Si to Ga is 97:3, and Si is rich in the nanowire. The EDX results from different nanowires further manifest that the distribution of Ga inside the nanowires with the absence of oxygen is nearly uniform and the Ga content of a nanowire is 3 at.%. The SAED pattern (right upper inset) indicates that the nanowire is single crystal hexagonal structure α-Si_3N_4 ($a = 7.765$ Å, $c = 5.627$ Å) with a growth direction of [110], which is in agreement with the XRD results. The EDX analyses of spear-like tips indicate that they contain Ga more than the nanowires. The

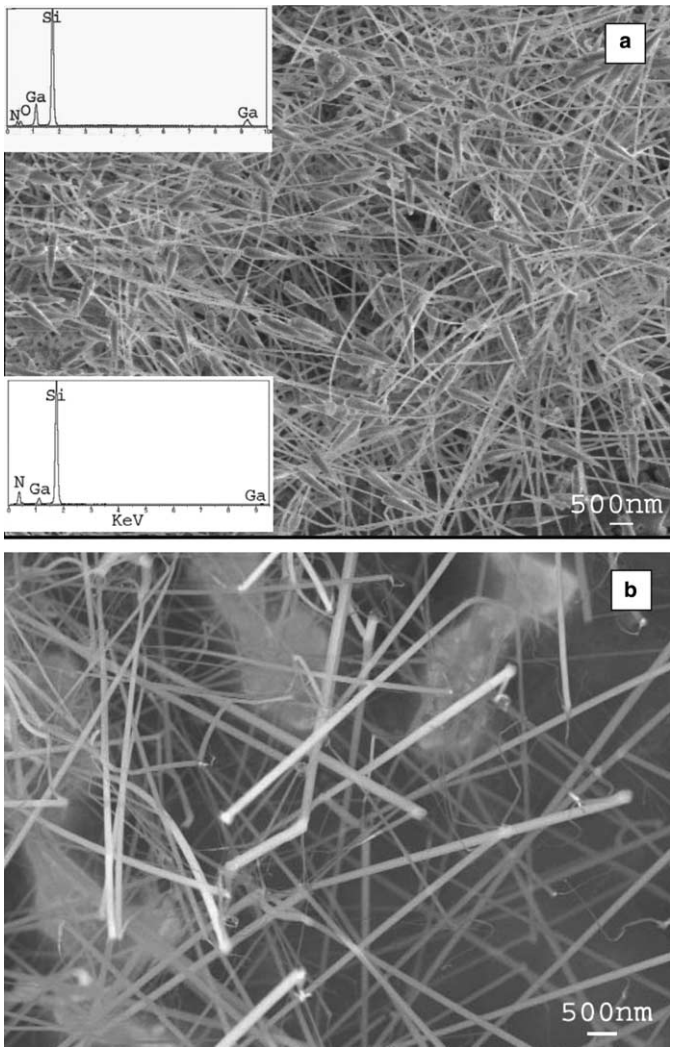

Fig. 1. (a) SEM image of the samples grown on a silicon substrate with GaN. The insets are EDX. (b) SEM image of as-prepared samples grown on an Au-coated silicon substrate without GaN.

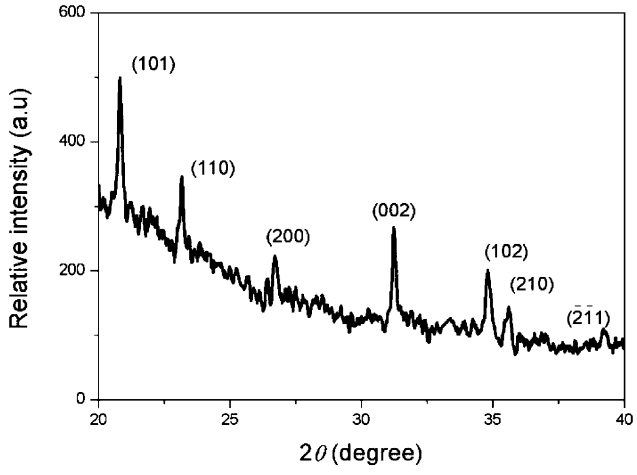

Fig. 2. XRD pattern of the as-prepared sample grown on a Si substrate with GaN.

SAED pattern (left upper inset) can be clearly indexed to single crystal with hexagonal α-Si_3N_4. No second pattern was observed, indicating that Ga is doped into α-Si_3N_4.

The TEM image of a nanocable is shown in Fig. 3(b). The diameter of the nanocable is about 60 nm and that of the core is about 15 nm. EDX analyses (inset) indicate that the atomic ratio of Si, N, O and Ga is 54:34:11.5:0.5, and the atomic ratio of Si to Ga 99.2:0.8. The Ga content in the nanocable is much less than that of Ga-doped Si_3N_4 nanowires. SAED analysis (inset) shows that the core is single crystal hexagonal α-Si_3N_4 with the growth direction along [1 1 0], whereas the sheath is amorphous phase, which is probably either silicon oxynitride or silica. A detailed discussion is given below.

Fig. 3(c) shows a corresponding HRTEM image of the nanocable (Fig. 3(b)). The HRTEM image clearly proves that the sheath is amorphous and the core is single crystal, which is consistent with the above SAED results. Hence, we can infer that the Ga-doped Si_3N_4 nanowire firstly forms and that then its outer layer is oxidized.

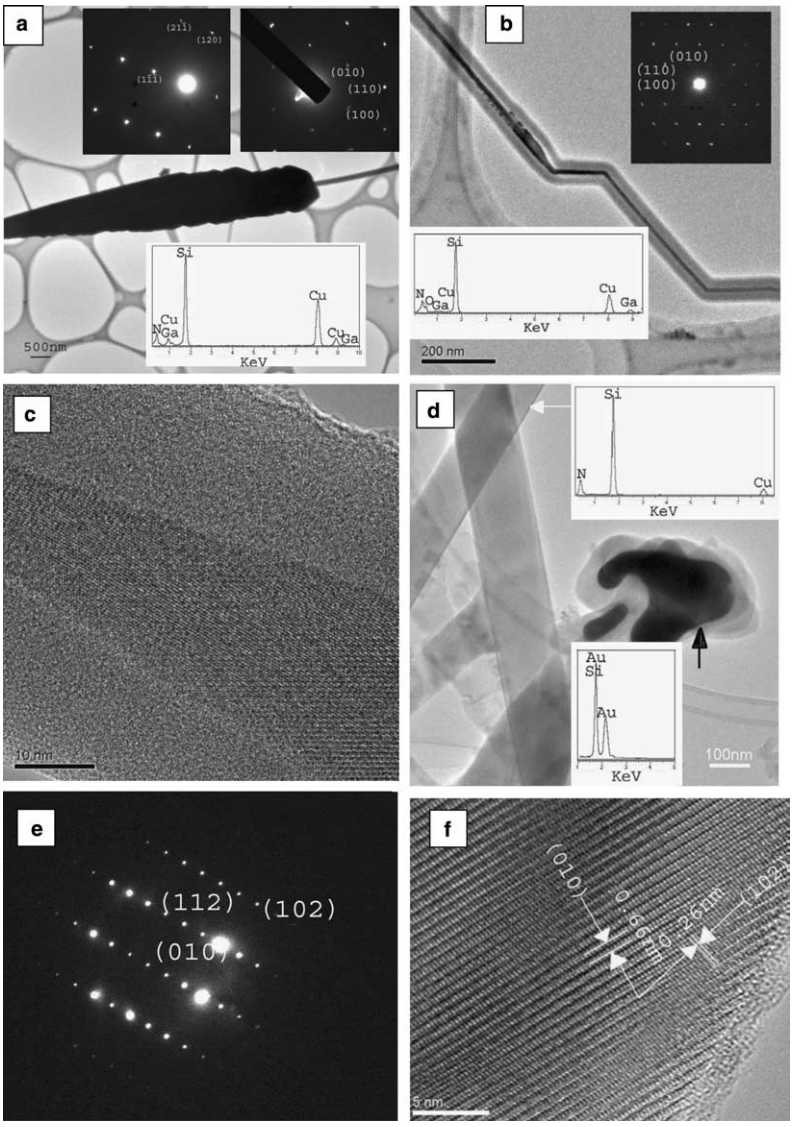

Fig. 3. (a) TEM image of a nanowire with a spearlike tip grown on a Si substrate with GaN. The lower inset is its EDX, and the left upper inset the SAED of the spearlike tip, and the right upper inset SAED of the nanowire. (b) TEM image of a nanocable, upper inset is its SAED, and lower inset is its EDX. (c) A high-resolution TEM image of the nanocable in (b). (d)–(f) are TEM, SAED and HRTEM of the nanowires grown on an Au-coated Si substrate without GaN, respectively.

Fig. 3(d)–(f) are the TEM, SAED and HRTEM images of the nanowires grown on an Au-coated Si substrate without GaN under the same conditions as that grown on the pure silicon substrate. EDX analysis at the position as indicated by the white arrow (upper inset in Fig. 3(d)) shows that it is composed of Si and N with the atomic ratio of 65:35, and no oxygen is detected. The tip (as indicated by the black arrow) is Au–Si alloy, as shown by the EDX (lower inset). The SAED pattern in Fig. 3(e) indicates that the nanowire is single crystal α-Si_3N_4 with a hexagonal structure and has a growth direction of [1 1 2]. The HRTEM image in Fig. 3(f) shows clearly atomic layers with a spacing of 0.66 nm and 0.26 nm, which corresponds to the (0 1 0) and (1 0 2) planes of hexagonal α-Si_3N_4, respectively. In particular, the amorphous layer around the edge of the atomic layer is very thin, implying that the Si_3N_4 nanowire is not easily oxidized.

In order to clarify the composition of the sheath, the line scan EDX analyses of a nanocable with an outer diameter (sheath) of 200 nm and inner diameter (core) of 50 nm have been carried out (Fig. 4). Si has broad peaks and maximum at the center. Nitrogen has also a broad peak; however, it has two stronger peaks near the outer layer, indicating a higher concentration in the sheath region. The above results are consistent with the previous observation for silicon oxynitride films [18–21]. As is seen, oxygen has a minimum around the central position, illustrating that the oxygen is mainly incorporated into amorphous silicon oxynitride. Ga

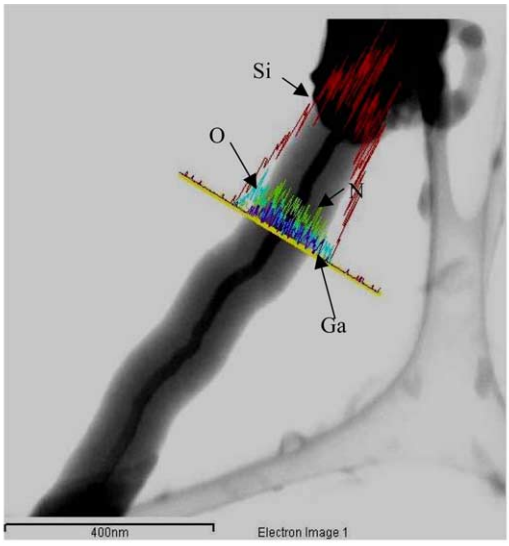

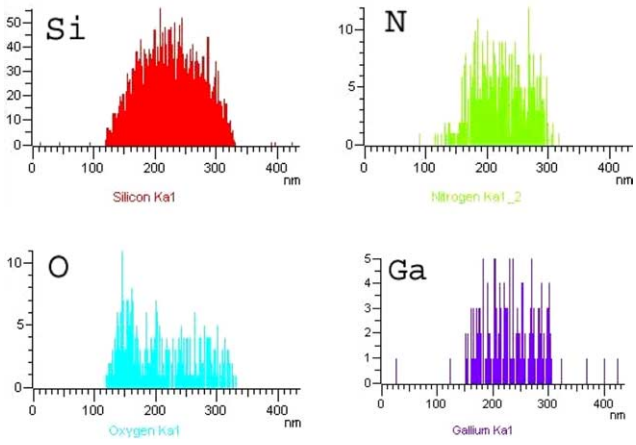

Fig. 4. The line-scan EDX analyses of a nanocable.

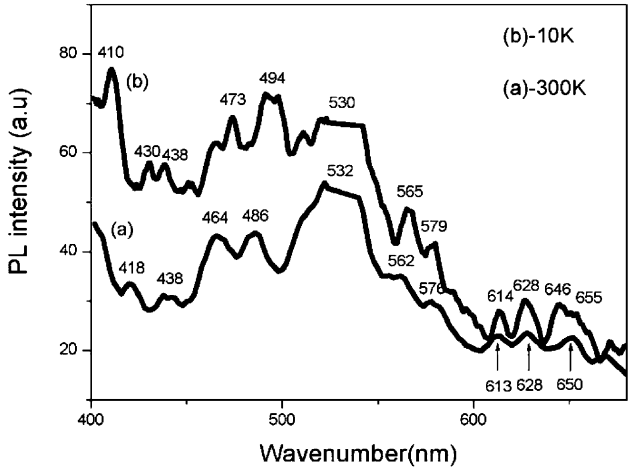

Fig. 5. Photoluminescence of Ga doped α-Si_3N_4 based nanowires.

has a broad distribution across the nanowire. These results clearly confirm that the nanocable has a good axial symmetry in composition and that the core is Ga-doped silicon nitride, and also clarify that the amorphous layer consists of Si, O, N and Ga; that is, the sheath is Ga-silicon oxynitride instead of pure SiO_2.

Fig. 5 shows the PL spectra of Ga-doped α-Si_3N_4 nanowires at 10 K and 300 K. Ten emission bands were observed around 418 (2.96 eV), 438 (2.83 eV), 464 (2.67 eV), 486 (2.55 eV), 532 (2.33 eV), 562 (2.20), 576 (2.15 eV), 613 (2.01 eV), 628 (1.97 eV), and 650 (1.90 eV) at 300 K. As the temperature decreased, the PL intensity increased and the bandwidth became slightly narrower. In the case of α-Si_3N_4 nanobelts, only a broad band from 420 to 750 nm with a maximum centered at 575 nm was observed [11]. Actually, the silicon nitride crystallite is inherently imperfect: electronic structure and spectral properties of Si_3N_4 exhibit the existence of Si dangling bonds between N_3 and Si, and N dangling bonds between Si_2 and N [22,23]. These point defects comprise an unpaired electron localized on a two-coordinated N and on a three-coordinated Si atom, which can result in different states. The EDX confirms that Si is rich in our sample. On the other hand, multiple emission bands of nanosized silicon nitride solids and films have been reported [23,24]. According to the theoretical calculations by Robertson et al. [25] the broad band centered on 532 nm (2.33 eV) can be attributed to electronic transition from Si^0 to N^{-1}, and the peaks of 532, 562, 576, 613, 628, and 650 nm can also be assigned to electronic transition between the conduction band and defect levels caused by Si and N dangling bonds. The peak around 418 nm (2.96 eV) arises from the N–Si–O bond. The emission at 532 nm (2.33 eV) may originate from the inner Ga-doped silicon nitride, similar to previously reported results on silicon nitride solid and film [23,24], while outer amorphous Ga-doped silicon oxynitride layers mainly contribute to the luminescence at 628 nm (1.97 eV), similar to previously reported results on amorphous silicon nitride/silica coaxial nanotubes [26]. In addition, the Ga emission peak at 522 nm (2.37 eV) [27] lies in the range of the Si^0 to N^{-1}) transition emission centered at 532 nm (2.33 eV); the Ga emission is not clearly resolvable. However, the broad peak center at 532 nm is obviously asymmetrical; it is more likely caused by Ga emission, which is a sharp peak at 522 nm [27]. The peaks at 464 and 486 nm result from Si–O–Si [24] and the emission band at 438 nm (2.83 eV) may be related to the oxidation process. The narrowing of the emission bands with the decrease in temperature is attributed to the reduction of Si and N defects.

To shed some light on the growth of Ga-doped Si_3N_4 nanowires and nanocables, we investigated the effect of the growth parameters (such as the flow rate of carrier gas and the reaction chamber pressure) on the growth of nanostructures. With an unvarying flow rate of ammonia, Ga concentration in silicon nitride increases

as the reaction chamber pressure increases; with constant reaction chamber pressure, when the flow rate of ammonia is less than 15 sccm, only SiO_2 nanostructures were observed instead of Si_3N_4 nanowires and/or SiO_xN_y nanostructures. Accordingly, Ga concentration varies with the reaction chamber pressure, and the nitrogen in nanowires and nanocables mainly come from NH_3 instead of GaN. It is noteworthy that neither nanocables nor oxygen elements were observed in the nanowires grown on the Au-coated Si substrates, implying that the nanowires grown on an Au coated Si substrate are not easily oxidized in comparison with the nanowires on a pure Si substrate. Moreover, the Ga content in the Ga-doped silicon nitride nanowires is more than that in the nanocables. As we know, gold is not easily oxidized. In contrast, gallium has a very strong ability to absorb oxygen from the leakage of the system and/or residual oxygen. The following reactions may be involved around 980 °C:

$$4Ga + 3O_2 \rightarrow 2Ga_2O_3 \ (1414\ \text{kJ/mol}) \quad (1)$$

$$Si + O_2 \rightarrow SiO_2 \ (685\ \text{kJ/mol}) \quad (2)$$

$$4Ga + O_2 \rightarrow 2Ga_2O \ (419\ \text{kJ/mol}) \quad (3)$$

$$4Ga + Ga_2O_3 \rightarrow 3Ga_2O \ (603\ \text{kJ/mol}) \quad (4)$$

$$2Ga_2O + Si \rightarrow SiO_2 + 4Ga \ (256\ \text{kJ/mol}) \quad (5)$$

The free energy change (−1414 kJ/mol) of reaction (1) is more than twice than that (−685 kJ/mol) of reaction (2), indicating that Ga absorbs oxygen more easily than Si. For reaction (5), the standard free energy change is −256 kJ/mol, and the reaction should therefore proceed. Hence, Ga can absorb O and then transfer it to Si and finally form silicon oxynitride sheathes, whereas Au can not do so. This phenomenon is similar to the formation of SiO_2 nanowires on the silicon substrate using GaN as the source of Ga catalyst [28]. The reason why the Ga content in the nanocable is smaller than that in the Ga-doped silicon nitride nanowires is not clear, demanding further investigation.

4. Summary

In conclusion, Ga-doped silicon nitride nanowires sheathed with amorphous silicon oxynitride have been fabricated on a silicon substrate using GaN to supply Ga. It turns out that the Ga is useful for the formation of an amorphous silicon oxynitride sheath. The PL spectrum of Ga-doped α-Si_3N_4 nanowires reveals 10 emission bands around 418, 438, 464, 486, 532, 562, 576, 613, 628, and 650 nm at 300 K, which are likely to be associated with electronic transition between the conduction band and defect states rather than the conduction band to valence band. As-grown Ga-doped Si_3N_4 nanowires and nanocables are expected to be useful in CMOS-based nanodevice.

Acknowledgements

The authors greatly appreciate financial support from the electron Spin Science Center (eSSC), the Korean Science and Engineering Foundation (KOSEF) and the Brain Korea 21 Project in 2004. We are also indebted to Dr. Zhu Yinbang for helpful discussions.

References

[1] Kim JH, Chung KW. J Appl Phys 1998;83:5831.
[2] Li WT, McKenzie DR, Mcfall WD, Zhang QC. Thin Solid Films 2001;384:46.
[3] Liu AY, Cohen ML. Phys Rev B 1990;41:10727.
[4] Zanatta AR, Nunes LAO. Appl Phys Lett 1998;72:3127.
[5] Matsuoka T, Taguchi S, Ohtsuka H, Taniguchi K, Hamaguchi C, Kakimoto S, et al. IEEE Electron Dev 1996;43:1364.
[6] Hao MY, Chen WM, Lai K, Lee JC, Gardner M, Fulford J. Appl Phys Lett 1995;66:1126.
[7] Okada Y, Tobin PJ, Rushbrook P, Dehart WL. IEEE Trans Electron Dev 1994;41:191.
[8] Fukuda H, Arakawa T, Ohno S. Jpn J Appl Phys 1990;29:L2333.
[9] Alessandri M, Clementi C, Crivelli B, Ghidini G, Pellizzer F, Martin F, et al. Microelectr Eng 1997;36:211.
[10] Matsoka T, Taguchi S, Ohtsuka H, Taniguchi K, Hamaguchi C, Kakimoto S, et al. IEEE Trans Electron Dev 1996;43:1364.
[11] Yin L, Bando Y, Zhu Y, Li Y. Appl Phys Lett 2003;83:3584.
[12] Wu XC, Song WH, Zhao B, Huang WD, Pu MH, Sun YP, et al. Solid State Commun 2000;115:683.
[13] Han W, Fan S, Li Q, Gu B, Zhang X, Yu D. Appl Phys Lett 1997;71:2271.
[14] Brown DM, Gray PV, Heumann FK, Philipp HR, Taft EA. J Electrochem Soc 1968;115:311.
[15] Bhat M, Han LK, Wristers D, Yan J, Kwong DL, Fulford JJ. Appl Phys Lett 1995;66:1225.
[16] Hattangady SV, Niimi H, Lucovsky G. Appl Phys Lett 1995; 66:3495.
[17] Hill WL, Vogel EM, Misra V, Mclarty PK, Wortman JJ. IEEE Trans Electron Dev 1996;43:15.
[18] Carr EC, Ellis KA, Buhrman RA. Appl Phys Lett 1995;66:1492.
[19] Park DS, Choi HJ, Han BD, Kim HD, Lim DS. J Mater Res 2002;9:2275.
[20] Chien FSS, Chang JW, Lin SW, Chou YC, Chen TT, Gwo S, et al. Appl Phys Lett 2000;76:360.
[21] Taguchi S, Ribeiro S. J Mater Proc Technol 2004;147:336.
[22] Pacchioni G, Erbetta D. Phys Rev B 1999;60:12617.
[23] Mao CM, Zhang L, Xie C, Wang T. J Appl Phys 1993;73:5185.
[24] Liu Y, Zhou Y, Shi W, Zhao L, Sun B, Ye T. Mater Lett 2004;58: 2397.
[25] Robertson J, Powell MJ. Appl Phys Lett 1984;44:856.
[26] Li YB, Bando Y, Golberg D, Uemura Y. Chem Phys Lett 2004; 393:128.
[27] Seto S, Mochida N, Inabe K, Suzuki K, Kuroda T, Minami F. Phys Status Solid (a) 2002;229:587.
[28] Pan ZW, Dai ZR, Ma C, Wang ZL. J Am Chem Soc 2002;124: 1817.